

This Page Is Inserted by IFW Operations  
and is not a part of the Official Record

## **BEST AVAILABLE IMAGES**

Defective images within this document are accurate representations of the original documents submitted by the applicant.

Defects in the images may include (but are not limited to):

- BLACK BORDERS
- TEXT CUT OFF AT TOP, BOTTOM OR SIDES
- FADED TEXT
- ILLEGIBLE TEXT
- SKEWED/SLANTED IMAGES
- COLORED PHOTOS
- BLACK OR VERY BLACK AND WHITE DARK PHOTOS
- GRAY SCALE DOCUMENTS

**IMAGES ARE BEST AVAILABLE COPY.**

**As rescanning documents *will not* correct images,  
please do not report the images to the  
Image Problem Mailbox.**

# LASER RAMAN SCATTERING AS A PROBE OF PROTEIN STRUCTURE

♦956

*Thomas G. Spiro*

Department of Chemistry, Princeton University, Princeton, New Jersey 08540

*Bruce P. Gaber*

Department of Chemistry, University of Oregon, Eugene, Oregon 97403

---

## CONTENTS

PERSPECTIVES AND SUMMARY .....	554
INTRODUCTION .....	555
RAMAN SPECTRA AND PROTEIN CONFORMATION .....	556
<i>Peptide Backbone</i> .....	556
<i>Side Chains</i> .....	560
<i>Disulfide</i> .....	560
<i>Aromatics</i> .....	560
<i>Applications</i> .....	561
RESONANCE RAMAN PROBES OF CHROMOPHORIC SITES .....	562
$\pi \rightarrow \pi^*$ <i>Chromophores</i> .....	563
<i>Rhodopsin</i> .....	563
<i>Heme proteins</i> .....	564
<i>Chlorophylls</i> .....	565
<i>Vitamin B-12</i> .....	565
<i>Ultraviolet chromophores</i> .....	565
<i>Metal Ion Sites</i> .....	566
<i>Iron-sulfur proteins</i> .....	566
<i>Transferrin</i> .....	567
<i>Hemerythrin</i> .....	567
<i>Hemocyanin</i> .....	568
<i>"Blue" copper proteins</i> .....	568
<i>Resonance Raman Labels</i> .....	569

553

## PERSPECTIVES AND SUMMARY

The Raman spectrum of a protein shows a series of peaks, characteristic of the molecular groupings present, whose frequencies are sensitive to local structural influences. While Raman intensities are intrinsically low, good quality protein spectra can be obtained with modern Raman spectrometers equipped with laser light sources. The sample can be studied in any physical state; protein spectra are obtainable *in situ* in biological materials, although background scattering and fluorescence from other components may interfere. The increasing tunability of laser sources makes possible the systematic exploitation of resonance Raman spectroscopy, in which the laser is tuned to an absorption band of the sample. Large enhancements are observed for certain Raman bands of the chromophore.

The instrumentation for normal and resonance Raman spectroscopy is the same, although the latter requires special precautions associated with side effects of light absorption. The information content is quite different, however. The normal Raman spectrum contains all of the active vibrational modes of the molecule (those associated with a change in molecular polarizability). These modes coalesce into recognizable bands for repeating structural units, i.e. peptide links and side chains of a given type. The normal Raman spectrum can therefore be used to study secondary and tertiary structure in proteins. In resonance Raman spectroscopy, enhancement of chromophore vibrations insures that they dominate the spectrum. Often they are the only features observable. Information about nonchromophoric parts of the protein is lost. What is gained, however, is a large increase in sensitivity and selectivity for vibrations of the chromophoric group. They can be monitored at high dilution or in complex mixtures. If, as is often the case, the chromophore is itself a site of biochemical activity, then the resonance Raman spectrum can be used to probe associated structural changes.

While normal and resonance Raman spectra show dramatic differences, there is actually a continuum of spectra between the two limiting cases. Pre-resonance enhancement is observed well outside of the absorption band proper. For example, the high relative intensities of ring vibrations of aromatic residues, in Raman spectra excited in the visible region, is associated with proximity to their ultraviolet absorption bands. In principle, one can adjust the selectivity of the Raman spectrum by tuning the laser to different parts of the electronic spectrum. This potential is currently limited by the tuning range of practical laser sources, which is expanding steadily.

## INTRODUCTION

Dr. Bull: What future do you hold out for the study of proteins by this technique?

Dr. Edsall: I believe there is hope for the study of proteins, but it is extremely difficult. . . .

Cold Spring Harbor, 1938 (1)

Twenty years elapsed before Professor Edsall's guarded optimism was rewarded with a "quite faint" 18-line photographic Raman spectrum of lysozyme (2); it was to be another ten years before Tobin (3) reported the first laser-excited spectra of lysozyme, pepsin, and  $\alpha$ -chymotrypsin. Within two years of Tobin's note the pioneering papers by Lord & Yu (4, 5) appeared. These papers detailed the spectra of lysozyme, ribonuclease, and chymotrypsin, emphasizing structural interpretations, and provided much of the impetus and direction for ensuing Raman studies of proteins. Also in 1970 Rimai and co-workers showed that resonance Raman (RR) spectra of carotene and lycopene can be obtained in situ in carrot and tomato tissue (6) and, in addition, produced the first RR spectrum of rhodopsin in frozen bovine retina (7). At the same time Long & Loehr (8) reported the first RR spectrum of a metalloprotein, rubredoxin. In 1972, RR spectra of hemoglobin and cytochrome *c* were published (9-11), setting in motion numerous RR studies of heme proteins and metalloporphyrins.

The procedure of Raman studies is to obtain and assign frequencies associated with molecular vibrations of interest. The interpretation of vibrational frequencies in terms of atomic masses, bond distances, and bond angles has firm theoretical and empirical underpinnings from extensive studies of small molecules (12-14). Since many vibrational modes are fairly well localized on specific groups of atoms, extension of the method to large molecules is straightforward, although complex. The potential for providing important information on biomolecular structure is high.

Two forms of spectroscopy, infrared and Raman, are capable of providing the needed data. Infrared spectroscopy involves direct absorption of light at frequencies appropriate for molecular vibrations. Since water is a strong absorber of infrared radiation over much of the spectral range of interest, the use of infrared spectroscopy in biological studies is limited, although several important applications, utilizing "window" regions of the water spectrum, have been reported (15-19). Raman spectroscopy involves a scan of the frequency of scattered light using a high-energy monochromatic source. Energy can be transferred to a vibrational transition of

the sample, with a corresponding frequency shift of the scattered photons. This is a low-probability event and a large incident photon flux is required to produce detectable Raman signals. In the pre-laser days, heroic measures were needed to provide such a flux, usually via gas-discharge lamps surrounding the sample. Large volumes of optically transparent material were required, severely constraining the applicability of the technique. Introduction of the laser, with its highly concentrated beam of light, dramatically relaxed these constraints. It is now possible to obtain a Raman spectrum of microliters of sample in any physical state (20, 21). Water is a weak Raman scatterer and produces minimal interference in aqueous medium studies.

The following sections summarize selected results of recent protein Raman studies. The field is burgeoning, and it is impossible in the space available to provide a comprehensive review. We hope instead to give some flavor for the kinds of information available and the potential for future work. More detailed reviews of both normal (22) and resonance Raman (23) work in this area have recently been published. As mentioned in the summary, quite different information emerges from these two approaches, yet the potential exists for combining them by appropriate laser tuning. The recent investigation by Shimanouchi and co-workers (24) of pre-resonance enhancement of peptide modes, using a series of visible and ultraviolet laser lines, is an apt example.

## RAMAN SPECTRA AND PROTEIN CONFORMATION

Although the vibrational modes of a protein are exceedingly numerous, a normal protein Raman spectrum shows consistent and recognizable peaks, as illustrated for carbonic anhydrase in Figure 1. The peak intensities depend on the number of repeating vibrational units in a given chemical environment, and on the change in molecular polarizability associated with the vibration. Both the peptide backbone and the amino acid side chains contribute. Assignment of the bands rests on extensive comparisons with amino acid and peptide spectra (4, 5, 22). Some of the bands have been found empirically to be sensitive, with respect to frequency and/or intensity, to conformational changes. These are summarized in Table 1, and a brief discussion is given below.

### *Peptide Backbone*

Of the vibrational modes associated directly with the amide bond, two have sufficient Raman intensity to be generally useful. Amide I, occurring in the region  $1630\text{--}1690\text{ cm}^{-1}$ , involves peptide  $\text{C}=\text{O}$  stretching primarily, while amide III, at  $1225\text{--}1275\text{ cm}^{-1}$ , has contributions from both  $\text{C-N}$  stretching

of the scattered photons. A high photon flux is required. For days, heroic measures with gas-discharge lamps surmounting the transparency of the material were the technique. Introduction of a laser source of light, dramatically increasing the Raman spectrum (20, 21). Water is a weak scatterer in aqueous medium.

Results of recent protein Raman spectroscopy are impossible in the space of time to give some idea of the potential for future developments in resonance Raman (23) as mentioned in the summary. These two approaches, yet to be combined with appropriate laser tuning. The results (24) of pre-resonance Raman spectroscopy and ultraviolet laser

## CONFORMATION

are exceedingly numerous, a large number of recognizable peaks, Table 1. The peak intensities vary in a given chemical environment, the assignability associated with the amino acid side chains. Extensive comparisons with the assignments of the bands have been made on the basis of frequency and/or intensity, summarized in Table 1, and a

the amide bond, two have been assigned to amide I, occurring in the stretching primarily, while the other two from both C-N stretching

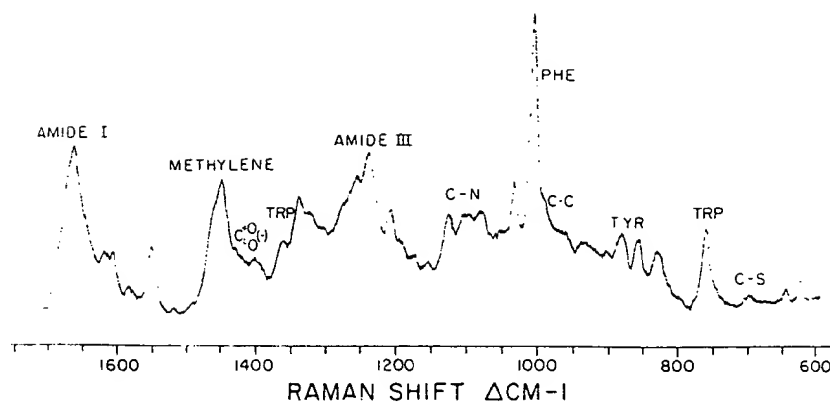


Figure 1 Laser Raman spectrum of a 14-mM solution of human carbonic anhydrase-B. Several modes useful in structural interpretation are identified (see Table 1).

and N-H in-plane bending. Model studies with homopolypeptides (22, 24-27) and proteins of well-defined structure (28-33) show that both frequencies are sensitive to peptide conformation, and establish the following assignments: anti-parallel  $\beta$ -pleated sheet,  $\sim 1670$   $\text{cm}^{-1}$  (I) and  $\sim 1235$   $\text{cm}^{-1}$  (III);  $\alpha$ -helix,  $\sim 1655$   $\text{cm}^{-1}$  (I); disordered structure,  $\sim 1665$   $\text{cm}^{-1}$  (I) and  $\sim 1245$   $\text{cm}^{-1}$  (III). The amide III frequency for the  $\alpha$ -helical conformation is still controversial. It had been thought to occur at  $\sim 1270$   $\text{cm}^{-1}$ , but both histidine and tyrosine contribute to this region (31). It is now clear that  $\alpha$ -helix is characterized by the absence of intensity below  $1275$   $\text{cm}^{-1}$  (25, 29) and by the presence of a strong band around  $1310$   $\text{cm}^{-1}$  (26, 30, 33), although the proximity of this band to overlapping  $\text{CH}_2$  deformation modes makes assignment difficult. Amide I falls in one of the few regions of the Raman spectrum where scattering from water interferes, and unequivocal assignment must be made in  $\text{D}_2\text{O}$ . The characteristic amide intensities for the different peptide structures have been related to parallel ultraviolet absorbance changes via a pre-resonance mechanism (35).

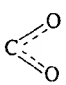
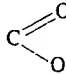
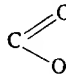
There is much interest in using the Raman spectrum for protein conformational analysis, by resolution of the amide I and III bands. Several attempts at quantitative estimation of secondary structure have been made (30, 33, 36). Lippert et al (33) report reasonable success ( $\pm 10$ -15% agreement with published values) using a procedure involving comparison of protein parameters (in both  $\text{H}_2\text{O}$  and  $\text{D}_2\text{O}$ ) with corresponding data for polylysine in its  $\alpha$ -helical,  $\beta$ -sheet, and random forms.

In addition to the amide modes, skeletal modes involving C-C ( $\sim 900$ - $1000$   $\text{cm}^{-1}$ ) and C-N ( $\sim 1100$   $\text{cm}^{-1}$ ) stretching are somewhat sensitive to

Table 1 Raman modes useful in the interpretation of protein structure

Origin and frequency ( $\Delta\text{cm}^{-1}$ )	Assignment	Structural information	References
<b>Backbone</b>			
<b>Skeletal Acoustic</b>			
25-30	Mode of large portion of protein; possibly inter-subunit mode	Overall structure; subunit interactions	39, 40
75	Torsion mode	$\alpha$ -helix (tentative)	40
160	Bending mode	$\beta$ -structure (tentative)	40
<b>Skeletal Optical</b>			
935-945 (950 $\text{D}_2\text{O}$ )	C-C stretch (or $\text{C}\alpha$ -C-N stretch)	$\alpha$ -helix	26, 30, 37, 29-31
900	C-C stretch	Conformational change markers broaden and lose intensity with denaturation	31, 38, 51
963	—	—	—
1002 ( $\text{H}_2\text{O}$ )	$\text{C}\alpha$ -C' or $\text{C}\alpha$ -C $\beta$ stretch	Suggestive of $\beta$ -pleated sheet	26
1012 ( $\text{D}_2\text{O}$ )	—	—	—
1100-1110	C-N stretch	Conformational change marker broadens and loses intensity with denaturation	51
<b>Amide I</b>			
	Amide C=O stretch	A sharp band suggests homogeneous structure and uniform hydrogen bonding. Strong hydrogen bonding lowers amide I frequencies	25, 26, 30, 67
1655 $\pm$ 5	—	$\alpha$ -helix	26
1632 ( $\text{D}_2\text{O}$ )	—	—	—
1670 $\pm$ 3	—	Antiparallel $\beta$ -pleated sheet	25, 26, 33
1661 $\pm$ 3 ( $\text{D}_2\text{O}$ )	—	—	26, 67
1665 $\pm$ 3	—	Disordered structure (solvated)	5, 67
1658 $\pm$ 2 ( $\text{D}_2\text{O}$ )	—	—	26, 30
1685	—	Disordered structure (non-hydrogen bonded)	29, 67
<b>Amide III</b>			
	N-H in-plane bend, C-N stretch	Strong hydrogen-bonding raises amide III frequencies	27
>1275	—	$\alpha$ -helix, no structure below 1275 $\text{cm}^{-1}$	25, 26, 30, 67
1235 $\pm$ 5 (sharp)	—	Antiparallel $\beta$ -pleated sheet	25, 26, 49, 67
983 $\pm$ 3 ( $\text{D}_2\text{O}$ )	—	—	26, 34
1245 $\pm$ 4 broad	—	Disordered structure	5, 26, 29
1235	—	Disordered structure (non-hydrogen-bonded)	29

Table 1 (Continued)

Amino Acid Sidegroups				
Tyrosine				
850/830 doublet	Fermi resonance between ring fundamental and overtone	State of phenolic -OH $I_{850}/I_{830} = 9:10$ to $10:7$ , "exposed" H-bond from acidic donor. $10:7$ to $3:10$ "buried," strong -OH H-bond to negative acceptor	50	
Tryptophan				
1361	Indole ring	Ring environment. Sharp intense line for buried residue. Intensity diminished on exposure or environmental change. Band contour of doublet near 1360-1380 is sensitive to environment	31, 51, 58	
1338	—	—	—	
Phenylalanine				
1006	Ring breath	Conformation-insensitive Frequency/Intensity reference	4, 5	
624	Ring breath	Ratio with tyrosine $664\text{ cm}^{-1}$ to estimate Phe/Tyr	67	
Histidine				
1409 ( $\text{D}_2\text{O}$ )	N-deuteroimidazole	Possible probe of ionization state, metalloprotein structure, proton transfer	5	
-S-S-				
510	S-S stretch	<i>gauche-gauche-gauche</i> . Broadening and/or shifts may indicate conformational heterogeneity among disulfides	45	
525	S-S stretch	<i>gauche-gauche-trans</i>	—	
540	S-S stretch	<i>trans-gauche-trans</i>	—	
C-S				
630-670	C-S stretch	<i>gauche</i>	45	
700-745	—	<i>trans</i>	—	
S-H				
2560-2580	S-H stretch	Environment, deuteration rate	67	
Carboxylic Acids				
1415	 stretch	State of ionization	4	
1730	 , C=O stretch		4	
	 , C=O stretch	Metal complexation	75	

in structure	References
information	
re; subunit inter-	39, 40
ive)	40
ntative)	40
	26, 30, 37
	29-31
il change mark-	31, 38,
and lose intensity	51
ation	
2-pleated sheet	26
—	
il change mark-	51
and loses intens-	
aturation	
suggests homogen-	25, 26,
re and form	30, 67
nding strong	
nding lowers	
uencies	26
—	—
pleated sheet	25, 26, 33
—	26, 67
ucture (solvated)	5, 67
—	26, 30
ucture (non-	29, 67
nded)	
gen-bonding raises	27
quencies	
ucture below	25, 26,
	30, 67
pleated sheet	25, 26, 49,
—	67
—	26, 34,
ucture	5, 26, 29
ucture	29
gen-bonded)	



conformation. A band at 935–945  $\text{cm}^{-1}$  appears common to helical structures (25, 29–31, 37, 38), while a band at  $\sim 1010 \text{ cm}^{-1}$  is considered suggestive of  $\beta$ -structure (25).

Proteins also have low-frequency "acoustical" modes, involving coherent vibrations of large portions of the molecule, which are highly sensitive to conformation. They have been observed in chymotrypsin and pepsin (39) and in lysozyme (40). The topic is the subject of an interesting review by Shimanouchi (41).

### Side Chains

Several of the more characteristic protein Raman bands are contributed by aromatic side chains or by disulfide links, the high relative intensity presumably arising from pre-resonance enhancement via the ultraviolet absorption bands of these groups.

**DISULFIDE** The suggestion by Lord & Yu (4) that the variation in S–S stretching frequency might be useful in determining disulfide dihedral angles in proteins has been a subject of lively debate (42–48). The currently accepted view (44, 46) is that  $\nu_{\text{S-S}}$  is *not* a direct function of S–S dihedral angle in the range 65–85°, but that some dihedral angle dependence may be evident for highly strained disulfides. The observed variations of  $\nu_{\text{S-S}}$  among alkyl disulfides have been explained by Sugeta (45, 46) as a consequence of vibrational coupling between S–S stretching and S–C–C bending modes. Thus  $\nu_{\text{S-S}}$  is sensitive to the conformation about the C–S bond, depending in particular upon conformations in which two hydrogens, one carbon and one hydrogen, or two carbons occupy positions *trans* to the distal sulfur across the C–S bond. These conformations, which may be denoted GGG (*gauche-gauche-gauche*), GGT (or TGG), and TGT, are associated (45) with  $\nu_{\text{S-S}}$  of 510  $\text{cm}^{-1}$ , 525  $\text{cm}^{-1}$ , and 540  $\text{cm}^{-1}$ , respectively, for aliphatic disulfides. Modifications of the Sugeta correlations have recently been proposed (48) that take account of substituent effects at the  $\beta$ -carbon and deviations from the strict *trans* and *gauche* conformations assumed by Sugeta.

In analogy to  $\nu_{\text{S-S}}$ , C–S stretching frequencies depend upon the conformation about the C–C bond adjacent to C–S (45): a *gauche* rotamer yielding  $\nu_{\text{C-S}} \sim 630\text{--}670 \text{ cm}^{-1}$  and a *trans* rotamer,  $\nu_{\text{C-S}} \sim 700\text{--}745 \text{ cm}^{-1}$ . Thus while disulfide and C–S modes are useful as indicators of protein –S–S– conformation, their utility is more limited and their interpretation considerably more complicated than heretofore realized.

**AROMATICS** Yu, Jo & O'Shea (49) proposed that the relative intensities of the tyrosine ring modes at 645  $\text{cm}^{-1}$ , 828  $\text{cm}^{-1}$ , and 853  $\text{cm}^{-1}$  could

common to helical structures.  $\nu_{\text{S-S}}$  is considered suggestive

of modes, involving coherent motions, which are highly sensitive to the environment (39). For a review by

bands are contributed by the relative intensity presumed from the ultraviolet absorption

that the variation in S-S stretching disulfide dihedral angles (42-48). The currently accepted function of S-S dihedral angle dependence may be observed variations of  $\nu_{\text{S-S}}$  (45, 46) as a consequence of S-C-C bending in the C-S bond, which has two hydrogens, one in *gauche* positions *trans* to the other, which may be TGG, and TGT, are at 540  $\text{cm}^{-1}$ , respectively, and correlations have been observed for substituent effects at the *gauche* conformations

depend upon the conformation of the *gauche* rotamer yielding 700-745  $\text{cm}^{-1}$ . Thus while the protein S-S conformation is considerably more

the relative intensities at 700  $\text{cm}^{-1}$  and 853  $\text{cm}^{-1}$  could

indicate whether the residue was "buried" or "exposed." In a joint study from the laboratories of Lord and Shimanouchi, Siamwiza et al (50) explored the proposal made by Yu et al and concluded the following: (a) the doublet near 830  $\text{cm}^{-1}$ /850  $\text{cm}^{-1}$  results from Fermi resonance between a fundamental and the first overtone of two ring modes; (b) the intensity ratio  $I_{850}/I_{830}$  is not sensitive to solvent polarity or backbone conformation, but rather is related primarily to the state of the phenolic OH; (c) in particular, a strong H-bond by -OH to a negative acceptor results in a low  $I_{850}/I_{830}$  ratio, whereas H-bonding between the phenolic oxygen and an acid donor yields a higher ratio; and (d) the ratio  $I_{850}/I_{830}$  is in the range 9 : 10 to 10 : 7 for exposed tyrosines, whereas for "buried" tyrosines it can be anywhere between 19 : 7 to 3 : 10.

Conformational aspects of certain modes from phenylalanine, tryptophan, and histidine are mentioned in Table 1.

### Applications

Protein Raman spectra have been used to monitor structural aspects of denaturation in lysozyme (31, 51-53),  $\beta$ -lactoglobulin (54), ribonuclease A (32, 55), tropomyosin (30), and insulin (29). Comparison of solution and crystal Raman spectra shows only minor changes for lysozyme (56), ribonuclease-A (57),  $\alpha$ -lactalbumin (37), basic pancreatic trypsin inhibitor (59), and carboxypeptidase A (57), but lyophilization of these proteins, and of chymotrypsinogen A and ovalbumin (60), results in significant changes both in main-chain and side-chain conformation. Angiotensin II displays the same antiparallel  $\beta$ -conformation in both solid state and concentrated aqueous solution (61). Bovine serum albumin (62), myosin (63), opsin (63a), and an antifreeze glycoprotein of an Antarctic fish (64) have been studied in solution.

Several snake venom proteins have been studied (34, 37, 66, 65). The neurotoxins show  $\beta$ -structure predominantly (34, 66, 65), whereas a cardiotoxin from the Mojave rattlesnake is mainly  $\alpha$ -helical (37). A sea anemone toxin, which is both neuro- and cardio-active, has a spectrum dominated by buried tryptophan, and a disordered backbone (66). Protein Raman spectra have been examined in lenses from both avian (38) and bovine (67) eyes. The avian protein is chiefly  $\alpha$ -helical, whereas the bovine protein has extensive  $\beta$ -structure. Scanning of individual locations of the bovine lens showed a uniform backbone structure but a definite variation in phenylalanine/tyrosine ratio. Two S-H stretches were detected, at 2582  $\text{cm}^{-1}$  and 2560  $\text{cm}^{-1}$ , suggesting different sulfhydryl environments. Prolonged oxidation showed only slight loss in  $\nu_{\text{S-H}}$  intensity, suggesting that the -SH groups are sufficiently restricted in their mobility that disulfide cross-links do not form.

Membrane proteins have been examined in erythrocyte ghosts (68, 69), sarcoplasmic reticulum (70), thymocyte plasma membrane (71, 71a), and transformed lymphocytes (72). Spectra of filamentous bacterial viruses (73) indicate that the coat proteins are  $\alpha$ -helical. The peptide ionophores valinomycin (74, 75) and gramicidin (76) have been examined, and changes on complexation observed. A conformation change from  $\beta$ -sheet toward disordered structure is observed when rabbit anti-ovalbumin is precipitated with its antigen (77).

### RESONANCE RAMAN PROBES OF CHROMOPHORIC SITES

Normal and resonance Raman spectra are obtained with the same spectrometer. The only requirement for RR spectroscopy is that the laser wavelength fall in or near the absorption band of interest. There are, however, experimental difficulties associated with the measurement of light scattering in an absorption band. These include absorption, heating, photoreactions, and fluorescence. Absorption requires an illumination geometry that minimizes the optical path through the sample, plus optimization of the concentration (78, 79). Laser-induced heating can be minimized by cooling the sample and by rotating (80) or circulating (81) it through the laser beam. Photoreactivity is a more difficult problem, but it has recently been demonstrated (82, 83) that Raman spectra can be obtained, even for highly photoactive species in a high-velocity stream. A sufficiently short transit time through the laser beam keeps the fraction of photolyzed sample to acceptable levels. Fluorescence is the most aggravating interference, since even low levels of photoemission can obscure the inherently weaker Raman scattering. Frequently luminescence arises from impurities, which can be removed by purification procedures or occasionally burned out by laser irradiation. Many, but by no means all, biological chromophores have acceptably low intrinsic fluorescence quantum yields, whereas in other cases addition of external quenching agents (e.g. sodium iodide) sometimes helps. Some improvement may be afforded by time-resolution of the detected light, since scattering is much faster than fluorescence. The needed instrumentation is still under development (84, 85). Perhaps the greatest promise for fluorescent systems comes from a new technique, coherent anti-Stokes Raman scattering (CARS) (86), in which the Raman signal is generated as a coherent beam of light, easily separated from the nondirectional fluorescence. Resonance enhancement can still be exploited, and resonance CARS spectra of dilute aqueous cytochrome *c* and vitamin B-12 have recently been obtained (87).

The advantage of RR spectroscopy for biological studies is that it offers a sensitive and selective probe of chromophore structure. Only certain

ocyte ghosts (68, 69),  
 membrane (71, 71a), and  
 bacterial viruses (73)  
 of ionophores valinomycin,  
 and changes on  
 $\beta$ -sheet toward disorder  
 is precipitated with

with the same species  
 that the laser wave-  
 length. There are, however,  
 several limitations of light scattering  
 for studying photoreactions,  
 such as geometry that mini-  
 mizes the concentration of the concen-  
 tration by cooling the  
 sample through the laser beam.  
 It has been demon-  
 strated even for highly photo-  
 labile short transit time  
 samples to accept  
 interference, since even  
 the weaker Raman  
 intensities, which can be  
 burned out by laser  
 chromophores have  
 whereas in other cases  
 (side) sometimes helps.  
 of the detected light,  
 needed instrumenta-  
 tion has the greatest promise for  
 coherent anti-Stokes Ra-  
 man scattering is generated as a  
 unidirectional fluores-  
 cence and resonance CARS  
 (12) have recently been

studies is that it offers  
 structure. Only certain

vibrational modes are enhanced, however. It is important to understand the enhancement pattern in order to make most effective use of the technique and to anticipate its limitation. The theory of RR scattering (88, 89) is complex, and is not reviewed here. It is possible, however, to draw from it a simple and useful generalization (90): significant enhancement can be expected for vibrational modes whose forms (normal coordinates) most closely resemble the distortions experienced by the molecule in the resonant excited state. Thus,  $\pi \rightarrow \pi^*$  transitions, which produce the dominant absorption bands of polyene and aromatic chromophores, show greatest enhancement for stretching vibrations of the  $\pi$  bonds, which are weakened in the excited state. Likewise, ligand  $\rightarrow$  metal charge-transfer transitions, often exhibited by metalloproteins, provide enhancement of the stretching vibrations of the ligand-metal bonds, which are weakened in the excited state, or of internal ligand vibrations, whose force constants are affected by the loss of the transferred electrons.

The frequencies of the observed RR bands are ground-state vibrational frequencies; only their intensities depend on the properties of the excited state. Biochemical events, e.g. ligand or substrate binding or protein conformation change, alter the vibrational frequencies only to the extent that the ground-state chromophore structure is distorted; such frequency shifts can be interpreted through the method of normal coordinate analysis (14). Intensity changes can occur without any ground-state distortion and are more sensitive monitors of chemical interactions, although structural interpretation is difficult.

### $\pi \rightarrow \pi^*$ Chromophores

**RHODOPSIN** The  $\pi \rightarrow \pi^*$  transitions of conjugated polyenes provide strong enhancement of Raman modes involving the skeletal vibrations of the carbon chain (91, 92). Good quality spectra can be obtained for rhodopsins, using dye laser excitation (93-95). For bacteriorhodopsin, whose photochemistry is reversible, it was possible to show, from the frequency of the C=N Schiff base link of the retinal chromophore, that the nitrogen atom is protonated in the ground state, but deprotonated in one of the photointermediates (94). This feature is plausibly related to the mechanism of the proton pump of the purple bacterial membrane. The irreversible photochemistry of mammalian rhodopsin makes it difficult to ascertain the exact composition of the sample in the laser beam. Oseroff & Callender (96) circumvented this problem by using low temperatures, where the photochemistry is reversible, and two laser beams, one to pump the sample to a particular stationary state composition and the other to generate the Raman spectrum. They were able to show that the Schiff base linkage of rhodopsin is protonated as previously suggested from work at higher temperature (93),

and that the first photointermediate, pre-lumirhodopsin, gives new Raman bands, in the  $\sim 800\text{ cm}^{-1}$  region, which are not characteristic of all-*trans* retinal. Good quality spectra of ground-state rhodopsin have been generated with rapid flow techniques (82, 83).

**HEME PROTEINS** Metalloporphyrins have two low-energy  $\pi \rightarrow \pi^*$  transitions. Because they interact strongly, the RR spectra contain a rich assortment of bands of different symmetry types, and quite detailed vibrational assignments can be made (97).

The most intense Raman bands arise from high-frequency ( $1100\text{--}1650\text{ cm}^{-1}$ ) porphyrin ring modes. Some of these display characteristic frequency shifts when the heme oxidation or spin state is changed. Back-donation of *d* electrons from low-spin FeII into the porphyrin  $\pi^*$  (antibonding) orbitals is relieved upon oxidation, or upon attachment of  $\pi$ -acid axial ligands, resulting in increased frequency for the "oxidation state" marker bands. The shifts for  $\text{O}_2$  binding to hemoglobin or myoglobin are fully as large as for oxidation to low-spin FeIII derivatives, suggesting that transfer of an electron from FeII to  $\text{O}_2$  is essentially complete (97, 98).

A switch from low- to high-spin FeII heme produces larger frequency decrements in a different set of bands, the "spin state" marker bands. These shifts are thought to result from loss in porphyrin  $\pi$ -conjugation accompanying the tilting of the pyrrole rings, as they follow the iron atom out of the plane, a movement that structural studies have firmly associated with the spin-state change (99, 100). This interpretation of the frequency shifts is supported by preliminary results of normal coordinate analysis (101). The observation that these shifts are the same for deoxyhemoglobin (Hb), deoxymyoglobin (Mb), and reduced horseradish peroxidase (HRP) and cytochrome *c'*, as well as for a protein-free five-coordinate FeII heme generated in solution (98), implies that the porphyrin conformation is the same in all of these instances, and that any molecular tension generated by the quaternary structural constraints in deoxyhemoglobin is not expressed in an increased doming of the porphyrin ring, as had been proposed (102).

On the other hand, the spin-state frequency shifts are observed to be significantly greater in the FeIII (met) forms of Hb and Mb than in HRP or cytochrome *c'* or protein-free FeIII hemes (98). From structural data on high-spin FeIII porphyrins (100), it appears that the doming that occurs in this oxidation state is slight, despite iron atom displacements that are nearly as large as for FeII. The extra shifts observed for Met-Hb and Mb suggest that the globin pocket resists relaxation of the deoxy porphyrin conformation. The implied strain in the resulting FeIII heme provides a structural basis for the inhibition of FeII heme oxidation, which is an essential characteristic of these  $\text{O}_2$  binding proteins.

psin, gives new Raman characteristic of all-*trans* opsin have been gener-

v-energy  $\pi \rightarrow \pi^*$  transition contain a rich assortment of detailed vibrational

frequency (1100–1650 cm<sup>-1</sup>) characteristic frequency of the Fe–O stretching mode. Back-donation of (antibonding) orbitals of  $\pi$ -acid axial ligands, in are fully as large as the transfer of an electron (7, 98).

duces larger frequency of the marker bands. These bands are conjugation accompanied by the iron atom out of the plane associated with the frequency shifts of the marker bands (101). The marker bands of hemoglobin (Hb), deoxyhemoglobin (Hb), deoxyhemoglobin (HRP) and cytochrome *c* heme generated by the quaternary structure are nearly the same in all cases (102).

is observed to be the same in Hb and Mb than in HRP. From structural data on the quaternary structure occurring in hemoglobin that are nearly the same in Hb and Mb suggest that the quaternary structure of the heme provides a structural basis for an essential charac-

The heme RR spectra also show weak low-frequency bands, some of which may involve Fe-ligand stretching (102a). These have yet to be analyzed in detail. The Fe–O stretching mode has been identified in oxy-Hb via <sup>18</sup>O<sub>2</sub> substitution (103). Its relatively high frequency, 567 cm<sup>-1</sup>, suggests an unusually strong bond, consistent with the short Fe–O distance found for the O<sub>2</sub> adduct of Collman's "picket fence" porphyrin (104). The Fe–F stretching mode of FeIII octaethylporphyrin fluoride has been identified at 595 cm<sup>-1</sup>, using the <sup>54</sup>Fe/<sup>56</sup>Fe isotope shift (105). This band does not appear in fluoro-met-Hb, presumably because the F<sup>-</sup> is weakly bound on the distal side of the out-of-plane heme. Axial ligand modes of bis-pyridine FeII heme are enhanced via resonance with an absorption band that is assignable to FeII  $\rightarrow$  pyridine charge transfer (98).

Protoheme proteins, such as Hb, Mb, HRP, and *b*-type cytochromes have peripheral vinyl substituents, conjugated to the porphyrin  $\pi$  system, which in *c*-type cytochromes are replaced by saturated thioether links to the protein. Protohemes show extra vinyl-induced RR bands (106), and their visible absorption bands are somewhat red-shifted. By adjusting the laser wavelength it is possible to excite selectively either cytochrome *c* or the *b* cytochromes in succinate-cytochrome *c* reductase (107). Cytochrome *c* oxidase contains heme *a*, which has a peripheral formyl as well as a vinyl group. Preliminary RR spectra show an extra band, at 1660 cm<sup>-1</sup>, in the reduced form of cytochrome oxidase, which is suggested to be the formyl C=O stretch (108).

**CHLOROPHYLLS** Chlorophylls *a* and *b* show many RR features reminiscent of the porphyrins (109, 110). The 9-keto C=O stretch is seen, and it shifts upon aggregate formation, as had been determined from infrared studies (110a). The RR spectra of chloroplasts, dominated by antennae chlorophyll, show several C=O components, suggesting varied environments. Preliminary spectra of bacterial photoreaction centers, as well as of bacteriochlorophyll and its pheophytin, have been reported (111).

**VITAMIN B-12** Cobalamins have RR spectra (112, 113) that are dominated by a single intense band near 1500 cm<sup>-1</sup>, reminiscent of polyenes, although many weaker features are observable. No changes of any significance are observed on changing the sixth ligand, among OH<sup>-</sup>, CN<sup>-</sup>, S<sub>2</sub>O<sub>3</sub><sup>2-</sup>, cysteinyl, methyl, and 5' deoxyadenosyl (coenzyme B<sub>12</sub>) (114). Reduction to CoII (B<sub>12r</sub>) or CoI (B<sub>12s</sub>) does produce substantial changes in relative intensities.

**ULTRAVIOLET CHROMOPHORES** The development of practical ultraviolet lasers holds promise of a major expansion in RR applications. It is

now possible to obtain usable power at 2573 Å by frequency doubling the 5145-Å argon laser line. RR spectra with this wavelength have been reported for adenine monophosphate and uridine monophosphate (115). Similar spectra should be obtainable for tyrosine and tryptophan, although fluorescence may present difficulties. Even amide modes are significantly enhanced (24) at 2573 Å, presumably via the  $\pi \rightarrow \pi^*$  transition at  $\sim 200$  nm.

### *Metal Ion Sites*

The characteristic colors of transition metal ions are usually associated with electronic transitions within the manifold of the valence  $d$  orbitals, the so-called " $d-d$ " or ligand field transitions. These are orbitally forbidden, and the absorption bands to which they give rise are weak. Resonance Raman enhancement is proportional to the oscillator strength of the electronic transition, and enhancement is expected to be weak for  $d-d$  scattering. Indeed centrosymmetric complexes have been shown to exhibit *de*-enhancement in  $d-d$  bands, due to interference effects (116). For noncentrosymmetric complexes, mixing in of  $p$  orbitals can significantly increase the oscillator strength. The most interesting biological examples are provided by  $\text{Co}^{2+}$ , which can substitute for  $\text{Zn}^{2+}$  (which, having a filled  $d$  sub-shell has no  $d-d$  transitions of its own) at the low-symmetry active sites of many zinc metalloenzymes, producing  $d-d$  bands in the red region of the spectrum with molar absorptivities of several hundred. A preliminary Raman study of  $\text{Co}^{2+}$  carboxypeptidase and carbonic anhydrase gave negative results (117), but in view of the significant resonance enhancement of Co-ligand stretching modes recently reported (118, 119) for simple tetrahedral  $\text{Co}^{2+}$  complexes, this application merits further study.

If the transition metal ion is easily reducible, and a bound ligand is easily oxidizable, then intense ligand  $\rightarrow$  metal charge-transfer transitions may occur in the visible or near-ultraviolet region. In biological systems these are observed for  $\text{Fe}^{3+}$  and  $\text{Cu}^{2+}$  complexes primarily, with ligands such as thiolate, phenolate, and peroxide. Several RR applications are described below.

**IRON-SULFUR PROTEINS** The iron-sulfur proteins contain  $\text{Fe}^{3+}$  and/or  $\text{Fe}^{2+}$  bound to thiolate (cysteine) and/or sulfide. Those forms containing one or more  $\text{Fe}^{3+}$  ions have intense absorption in the visible region, attributable to  $\text{S} \rightarrow \text{Fe}$  charge-transfer transitions. Resonance enhancement is therefore expected for S-Fe vibrational modes. This was first demonstrated (8, 120) for oxidized rubredoxin, which has one  $\text{Fe}^{3+}$  ion in somewhat distorted tetrahedral coordination by four cysteine side chains (121). The RR spectrum shows bands at 314 and 368  $\text{cm}^{-1}$  assigned to the symmetric and

frequency doubling the length have been rephosphate (115). Similarly, tryptophan, although modes are significantly transition at  $\sim 200$  nm.

usually associated with valence  $d$  orbitals, the  $d-d$  transitions are orbitally forbidden, and are weak. Resonance Raman scattering strength of the electronic transitions is weak for  $d-d$  scatterers, but has been shown to exhibit dependence on the nature of the ligands (116). For noncentrosymmetric complexes, a significant increase in Raman intensity is observed for examples are provided, having a filled  $d$  shell and symmetry active sites in the red region of the spectrum. Preliminary Raman studies have given negative results for the enhancement of Co(II) for simple tetrahedral complexes.

A bound ligand is easily transferred; transitions may be observed in biological systems these days, with ligands such as heme. Examples are described.

Complexes contain  $\text{Fe}^{3+}$  and/or  $\text{Fe}^{2+}$ . Those forms containing a visible region, attributable to the enhancement is there. The first demonstrated (8), in somewhat distorted octahedral sites (121). The RR spectrum is due to the symmetric and

nonsymmetric stretching modes of the  $\text{FeS}_4$  unit, and bands at 150 and 126  $\text{cm}^{-1}$ , possibly arising from bending modes.

Adrenodoxin is a member of the class of proteins that are thought to contain two iron atoms bridged by sulfide ions, and bound to the protein through two cysteine side chains, each iron atom again having a roughly tetrahedral  $\text{FeS}_4$  coordination group. The RR spectrum of oxidized adrenodoxin (122) shows three bands in the Fe-S stretching region, at 397, 350, and 297  $\text{cm}^{-1}$ . The first and last of these can be assigned to the bridging sulfides by virtue of their large shifts to lower frequency on replacement of sulfide by selenide.

Several proteins contain  $\text{Fe}_4\text{S}_4$  clusters, in which the iron and sulfur atoms are arranged at the alternating corners of an approximate cube, with each iron atom bound to a cysteine side chain. HiPIP (high-potential iron protein) (123) and bacterial ferredoxin (124) have been characterized by X-ray crystallography. Chemical analogs with a variety of thiolate ligands bound to the  $\text{Fe}_4\text{S}_4$  cluster have been prepared and characterized (125-127). Much physical evidence suggests that the dianionic form of these analogs is at the same oxidation level (formally  $\text{Fe}^{2.5+}$ ) as reduced HiPIP and oxidized ferredoxin. Preliminary RR spectra have been compared for these three species (128). The chemical analog (phenylsulfide derivative) shows two polarized bands, at 332 and 275  $\text{cm}^{-1}$ , assignable to symmetric stretching of terminal and bridging Fe-S bonds, respectively. In the protein spectra, the terminal Fe-S mode is split, implying inequivalence of the Fe-cysteine links. This structural feature is of interest in connection with the question of protein control of the redox potential.

**TRANSFERRIN** The serum transport protein, transferrin, avidly binds  $\text{Fe}^{3+}$  with the development of a strong absorption band centered at  $\sim 465$  nm. Both histidine and tyrosine side chains have been implicated as binding groups, and the visible absorption is attributable to phenolate  $\rightarrow$   $\text{Fe}^{3+}$  charge transfer (129). RR spectra (129-131) show several high-frequency modes, all of which can be assigned to phenolate ring modes, by comparison with the spectrum of a  $\text{Fe}^{3+}$  complex of an EDTA-like chelate with two phenolate binding groups (129).

**HEMERYTHRIN** Hemerythrin, the oxygen-carrying protein of marine worms, binds one  $\text{O}_2$  molecule per two iron atoms (132). The deoxy binding site contains  $\text{Fe}^{2+}$  ions, while the oxy site contains a pair of magnetically interacting  $\text{Fe}^{3+}$  ions, presumably generated by a reversible reduction of bound  $\text{O}_2$  to  $\text{O}_2^{2-}$ . This view has been confirmed by RR spectroscopy (133) where excitation in the visible absorption band of oxy-hemerythrin reveals



a Raman band at  $844\text{ cm}^{-1}$ , shifting to  $798\text{ cm}^{-1}$  on substitution of  $^{18}\text{O}_2$ , and therefore assignable to O-O stretching. The frequency is characteristic of peroxides. The Fe-O stretch is also observed at  $500\text{ cm}^{-1}$ , shifting to  $428\text{ cm}^{-1}$  on  $^{18}\text{O}_2$  substitution. Moreover, the mode of  $\text{O}_2$  binding has been shown to be unsymmetrical (presumably attachment to one or both Fe atoms is through only one of the O atoms) by use of the mixed isotopic molecule  $^{16}\text{O}^{18}\text{O}$  (133a). End-on binding of  $\text{N}_3^-$  is suggested for metazidohemerythrin by its RR spectrum (134), which reveals the asymmetric azide stretch to be at  $2049\text{ cm}^{-1}$ , close to the frequency  $2045\text{ cm}^{-1}$  found in the infrared spectrum of metazidohemoglobin (17).

**HEMOCYANIN** The oxygen carrier of arthropods and molluscs, hemocyanin, is a copper protein, but its chemistry is analogous to hemerythrin. Thus, one  $\text{O}_2$  molecule is bound per two Cu atoms, with concomitant oxidation from  $\text{Cu}^+$  to  $\text{Cu}^{2+}$ . Again RR spectroscopy (135, 136) demonstrates the presence of bound peroxide, with the O-O stretch located at  $742\text{ cm}^{-1}$  and shifting to  $704\text{ cm}^{-1}$  on  $^{18}\text{O}_2$  substitution. This mode is in resonance (136) with the visible absorption envelope at  $\sim 570\text{ nm}$ , assignable to  $\text{O}_2^{2-} \rightarrow \text{Cu}^{2+}$  charge transfer. Another mode, near  $280\text{ cm}^{-1}$  and attributable to Cu-imidazole stretching, is observed to be subject to pre-resonance enhancement by an intense near-ultraviolet transition at  $340\text{ nm}$  (136). Excitation directly into the  $340\text{-nm}$  band, using the  $351.1\text{-nm}$   $\text{Ar}^+$  laser line (137), produces a RR spectrum with several features below  $400\text{ cm}^{-1}$  in the  $\text{Cu}^{2+}$ -ligand region, but none at higher frequency where imidazole ring modes are expected. This observation militates against assignment of the near-ultraviolet transition to imidazole  $\rightarrow \text{Cu}^{2+}$  charge transfer (136) and favors assignment to a simultaneous pair excitation (138), which might be expected to enhance only vibrations localized on the  $\text{Cu}^{2+}$  ions.

**"BLUE" COPPER PROTEINS** Several copper proteins, e.g. azurin, stericacyanin, and plastocyanin, show intense absorption near  $600\text{ nm}$  in their oxidized form, giving them an unusually strong blue color. The multicopper oxidases, laccase and ceruloplasmin, also contain "blue" sites. Much recent evidence (139) points to cysteine  $\rightarrow \text{Cu}^{2+}$  charge transfer as the origin of the  $600\text{-nm}$  absorption band. Infrared data (140) implicate a peptide group in the  $\text{Cu}^{2+}$  coordination sphere, and NMR evidence points to the involvement of imidazole (141). RR spectra (142-144) show several bands near  $400\text{ cm}^{-1}$ . The region near  $400\text{ cm}^{-1}$  is appropriate for Cu-N and Cu-O stretching modes. Weak resonance enhancement is found (142) for higher-frequency modes identifiable with peptide group frequencies, consistent with the view that the  $\text{Cu}^{2+}$  ion is bound to peptide. The  $\sim 275\text{ cm}^{-1}$  band

substitution of  $^{18}\text{O}_2$ , and frequency is characteristic of  $500\text{ cm}^{-1}$ , shifting to  $428\text{ cm}^{-1}$  of  $\text{O}_2$  binding has been assigned to one or both Fe atoms of the mixed isotopic azide suggested for metazoids. The asymmetric azide band at  $2045\text{ cm}^{-1}$  found in the

has been assigned to  $\text{Cu}^{2+}$ -S stretching, and its weakness has been rationalized with orbital overlap arguments (143, 144). This frequency is also appropriate for  $\text{Cu}^{2+}$ -imidazole stretching, and it is conceivable that the Cu-S bond is unusually strong, so that its frequency falls in the  $\sim 400\text{ cm}^{-1}$  group of bands.

### Resonance Raman Labels

Many biological sites are not chromophoric and are not directly amenable to RR investigation. They can, however, be labelled with exogenous chromophores that can probe structural features via their RR spectra. Aromatic azo compounds with appropriate functionality have been used to probe hapten binding to antibodies (145) and inhibitor binding to carbonic anhydrase (146) and to trypsin (147). RR spectra of a chelating azo-dye, zincon, which is a competitive coenzyme inhibitor of liver alcohol dehydrogenase, have been interpreted as indicating binding to the active-site zinc ion through the azo and phenolic groups (148). RR spectra of 4-amino-2-nitro-3-transcinnaoyl  $\alpha$ -chymotrypsin, a stable intermediate, gave evidence of twisting about the C- $\text{NO}_2$  bond but no perturbation of the trans -C=C- conformation or the coplanar phenyl ring (149).

### ACKNOWLEDGMENTS

We thank Professors Scheraga, Lord, Lippert, Yu, and Harada for providing manuscripts prior to publication; Professor R. B. Martin and Dr. A. E. Van Wart for helpful discussions; and Mr. William Craig for obtaining the spectrum shown in Figure 1.

### Literature Cited

1. Edsall, J. T. 1938. *Cold Spring Harbor Symp. Quant. Biol.* 6:440-49.
2. Garfinkel, D., Edsall, J. T. 1958. *J. Am. Chem. Soc.* 80:3818-23.
3. Tobin, M. C. 1968. *Science* 161:68-69.
4. Lord, R. C., Yu, N. T. 1970. *J. Mol. Biol.* 50:509-24.
5. Lord, R. C., Yu, N. T. 1970. *J. Mol. Biol.* 51:203-13.
6. Gill, D., Kilponen, R. G., Rimai, L. 1970. *Nature* 227:743.
7. Rimai, L., Kilponen, R. G., Gill, D. 1970. *Biochem. Biophys. Res. Commun.* 40:422.
8. Long, T. V. II, Loehr, T. M., Allkins, J. R., Lovenberg, W. 1971. *J. Am. Chem. Soc.* 93:1809.
9. Strekas, T. C., Spiro, T. G. 1972. *Biochim. Biophys. Acta* 278:188-92.
10. Brunner, H., Mayer, A., Sussner, H. 1972. *J. Mol. Biol.* 70:153-56.
11. Spiro, T. G., Strekas, T. C. 1972. *Proc. Natl. Acad. Sci. USA* 69:2622-26.
12. Herzberg, G. 1945. *Infrared and Raman Spectra and Polyatomic Molecules*. Princeton, N.J.: Van Nostrand-Reinhold. 632 pp.
13. Colthup, N. B., Daly, L. H., Wiberley, S. E. 1975. *Introduction to Infrared and Raman Spectroscopy*. New York: Academic. 523 pp. 2nd ed.
14. Dollish, F. R., Fateley, W. G., Bentley, F. F. 1974. *Characteristic Raman Frequencies of Organic Compounds*. New York: Wiley. 443 pp.
15. Thomas, G. J. 1971. In *Physical Techniques in Biochemical Research*, ed. A. Weissberger, 1A: Chap. 4. New York: Academic. 2nd ed.
16. Riepe, M. E., Wang, J. H. 1968. *J. Biol. Chem.* 243:2779-87.
17. McCoy, S., Caughey, W. S. 1970. *Biochemistry* 9:2387-93.

inopods and molluscs, is analogous to heme-Cu atoms, with concomitant spectroscopy (135, 136) of the O-O stretch located at  $\sim 570\text{ nm}$ , assignable at  $280\text{ cm}^{-1}$  and attributed to pre-resonance excitation at  $340\text{ nm}$  (136). The  $351.1\text{-nm}$   $\text{Ar}^+$  laser line is at  $400\text{ cm}^{-1}$  in the region where imidazole ring stretching assignment of the  $\text{Cu}^{2+}$  ion is against assignment of the  $\text{Cu}^{2+}$  ion (136) and (138), which might be the  $\text{Cu}^{2+}$  ions.

proteins, e.g. azurin, stellerin near  $600\text{ nm}$  in their blue color. The multi-site "blue" sites. Much evidence points to the origin of the  $\text{Cu}^{2+}$  ion (140) implicate a peptide bond. The evidence points to the origin of the  $\text{Cu}^{2+}$  ion (140) show several bands for Cu-N and Cu-O stretching (142) for higher-frequencies, consistent with the  $\sim 275\text{ cm}^{-1}$  band

18. Barlow, C. H., Ohlsson, P.-I., Paul, K.-G. 1976. *Biochemistry* 15:2225-29
19. Alben, J. O., Bare, G. H., Bromberg, P. A. 1974. *Nature* 252:736-38
20. Gilson, T. R., Hendra, P. J. 1970. *Laser Raman Spectroscopy*. New York: Wiley-Interscience. 266 pp.
21. Tobin, M. C. 1971. *Laser Raman Spectroscopy*. New York: Wiley-Interscience
22. Frushour, B. G., Koenig, J. L. 1975. In *Advances in Infrared and Raman Spectroscopy*, ed. R. J. H. Clark, R. E. Hester, 1:35-97. London: Heyden. 301 pp.
23. Spiro, T. G., Loehr, T. M. 1975. See Ref. 22, pp. 98-142
24. Harada, I., Sugawara, Y., Matsuura, H., Shimanouchi, T. 1975. *J. Raman Spectrosc.* 4:91-98
25. Small, E. W., Fanconi, B., Peticolas, W. L. 1970. *J. Chem. Phys.* 52:4369-79
26. Yu, T.-J., Lippert, J. L., Peticolas, W. L. 1973. *Biopolymers* 12:2161-76
27. Chen, M. C., Lord, R. C. 1974. *J. Am. Chem. Soc.* 96:4750-52
28. Yu, N. T., Liu, C. S. 1972. *J. Am. Chem. Soc.* 94:5127-28
29. Yu, N. T., Liu, C. S., O'Shea, D. C. 1972. *J. Mol. Biol.* 70:117-32
30. Frushour, B. G., Koenig, J. L. 1974. *Biopolymers* 13:1809-19
31. Chen, M. C., Lord, R. C., Mendelson, R. 1974. *J. Am. Chem. Soc.* 96:3038-42
32. Chen, M. C., Lord, R. C. 1976. *Biochemistry* 15:1889-97
33. Lippert, J. L., Tyminski, D., Desmeules, P. J. 1976. *J. Am. Chem. Soc.* 98:7075-80
34. Yu, N. T., Lin, T. S., Tu, A. T. 1975. *J. Biol. Chem.* 250:1782-85
35. Painter, P. C., Koenig, J. L. 1976. *Biopolymers* 15:241-55
36. Pezolet, M., Pigeon-Gosselin, M., Coulombe, L., 1976. *Biochim. Biophys. Acta* 453:502-12
37. Tu, A. T., Prescott, B., Chou, C. H., Thomas, G. J. Jr. 1976. *Biochem. Biophys. Res. Commun.* 68:1139-45
38. Kuck, J. F. R. Jr., East, E. J., Yu, N. T. 1976. *Exp. Eye Res.* 22:1-6
39. Brown, K. G., Erfurth, S. C., Small, E. W., Peticolas, W. L. 1972. *Proc. Natl. Acad. Sci. USA* 69:1467-69
40. Genzel, L., Keilmann, F., Martin, T. P., Winterling, G., Yacoby, Y., Frohlich, H., Makinen, M. W. 1976. *Biopolymers* 15:219-25
41. Shimanouchi, T., 1976. In *Structural Studies of Macromolecules by Spectroscopic Methods*, ed. K. J. Ivin, pp. 59-72. New York: Wiley
42. Van Wart, H. E., Lewis, A., Scheraga, H. A., Saeva, F. D. 1973. *Proc. Natl. Acad. Sci. USA* 70:2619-23
43. Martin, R. B. 1974. *J. Phys. Chem.* 78:855-56
44. Van Wart, H. E., Scheraga, H. A., Martin, R. B. 1976. *J. Phys. Chem.* 80:1832
45. Sugeta, H., Go, A., Miyazawa, T. 1972. *Chem. Lett.* pp. 83-86
46. Sugeta, H. 1975. *Spectrochim. Acta* 31A:1729-37
47. Van Wart, H. E., Shipman, L. L., Scheraga, H. A. 1975. *J. Phys. Chem.* 79:1436-47
48. Van Wart, H. E., Scheraga, H. A. 1976. *J. Phys. Chem.* 80:1812-32
49. Yu, N. T., Jo, B. H., O'Shea, D. C. 1973. *Arch. Biochem. Biophys.* 156:71-76
50. Siamwiza, M. N., Lord, R. C., Chen, M. C., Takamatsu, T., Harada, I., Matsuura, H., Shimanouchi, T. 1975. *Biochemistry* 14:4870-76
51. Chen, M. C., Lord, R. C., Mendelsohn, R. 1973. *Biochim. Biophys. Acta* 328:252-60
52. Brunner, H., Sussner, H. 1972. *Biochim. Biophys. Acta* 271:16-22
53. Lord, R. C., Mendelsohn, R. 1972. *J. Am. Chem. Soc.* 94:2133-35
54. Frushour, B. G., Koenig, J. L. 1975. *Biopolymers* 14:649-62
55. Yu, N. T., Jo, B. H., Liu, C. S. 1972. *J. Am. Chem. Soc.* 94:7572-75
56. Yu, N. T., Jo, B. H. 1973. *Arch. Biochem. Biophys.* 156:469-74
57. Yu, N. T., Jo, B. H. 1973. *J. Am. Chem. Soc.* 95:5033-37
58. Yu, N. T. 1974. *J. Am. Chem. Soc.* 96:4664-68
59. Brunner, H., Holz, M. 1975. *Biochim. Biophys. Acta* 379:408-17
60. Koenig, J. L., Frushour, B. G. 1972. *Biopolymers* 11:2505-20
61. Fermandjian, S., Fromageot, P., Tistchenko, A. M., Leicknam, J. P., Lutz, M. 1972. *Eur. J. Biochem.* 28:174-82
62. Chen, M. C., Lord, R. C. 1976. *J. Am. Chem. Soc.* 98:990-92
63. Carew, E. B., Asher, I. M., Stanley, H. E. 1975. *Science* 188:933-36
- 63a. Rothschild, K. J., Andrew, J. R., De Grip, W. J., Stanley, H. E. 1976. *Science* 191:1176-78
64. Tomimatsu, Y., Scherer, J. R., Yeh, Y., Feeney, R. E. 1976. *J. Biol. Chem.* 251:2290-98
65. Harada, I., Takamatsu, T., Shimanouchi, T., Miyazawa, T., Tamiya, N. 1976. *J. Phys. Chem.* 80:1153-56
66. Prescott, B., Thomas, G. J. Jr., Beress,

- H. E., Lewis, A., Scheraga, H. A. 1973. *Proc. Natl. Acad. Sci. USA* 70:2619-23
- B. 1974. *J. Phys. Chem.*
- H. E., Scheraga, H. A., B. 1976. *J. Phys. Chem.* 80:
- Go, A., Miyazawa, T. 1972. pp. 83-86
1975. *Spectrochim. Acta*
- H. E., Shipman, L. L., A. 1975. *J. Phys. Chem.*
- I. E., Scheraga, H. A. 1976. *Chem.* 80:1812-32
- Jo, B. H., O'Shea, D. C. 1975. *Biochem. Biophys.* 156:
- I. N., Lord, R. C., Chen, M., Tsu, T., Harada, I., Matsushimaouchi, T. 1975. *Biochim. Biophys. Acta* 328:
- Lord, R. C., Mendelsohn, R. 1972. *Biochim. Biophys. Acta* 271:16-22
- Mendelsohn, R. 1972. *J. Soc.* 94:2133-35
- G., Koenig, J. L. 1975. *Appl. Spectrosc.* 29:146-152
- H., Liu, C. S. 1972. *Soc.* 94:7572-75
- B. H. 1973. *Arch. Biochem. Biophys.* 156:469-74
- B. H. 1973. *J. Am. Chem. Soc.* 95:37
1974. *J. Am. Chem. Soc.*
- Holz, M. 1975. *Biochim. Biophys. Acta* 379:408-17
- Frushour, B. G. 1972. *J. Am. Chem. Soc.* 94:2505-20
- S., Fromageot, P., Tist, L., Leicknam, J. P., Lutz, M. 1975. *J. Biochem.* 28:174-82
- Lord, R. C. 1976. *J. Am. Chem. Soc.* 98:990-92
- Asher, I. M., Stanley, H. E. 1976. *Science* 188:933-36
- K. J., Andrew, J. R., De Stanley, H. E. 1976. *Science*
- Scherer, J. R., Yeh, Y., E. 1976. *J. Biol. Chem.*
- akamatsu, T., Shimanouawa, T., Tamiya, N. 1976. *J. Am. Chem. Soc.* 98:1153-56
- Thomas, G. J. Jr., Beress, L., Wunderer, G., Tu, A. T. 1976. *FEBS Lett.* 64:144-147
- Yu, N. T., East, E. J. 1975. *J. Biol. Chem.* 250:2196-202
- Lippert, J. L., Gorczyca, L. E., Meiklejohn, G. 1975. *Biochim. Biophys. Acta* 382:51-57
- Wallach, D. F. H., Verma, S. P. 1975. *Biochim. Biophys. Acta* 382:542-51
- Milanovich, F. P., Yeh, Y., Baskin, R. J., Harney, R. C. 1976. *Biochim. Biophys. Acta* 419:243-50
- Verma, S. P., Wallach, D. F. H., Schmidt-Ullrich, R. 1975. *Biochim. Biophys. Acta* 394:633-45
- 71a. Schmidt-Ullrich, R., Verma, S. P., Wallach, D. F. H. 1976. *Biochim. Biophys. Acta* 426:477-88
- Schmidt-Ullrich, R., Verma, S. P., Wallach, D. F. H. 1975. *Biochem. Biophys. Res. Commun.* 67:1062-69
- Thomas, G. J. Jr., Murphy, P. 1975. *Science* 188:1205-7
- Rothschild, K. J., Asher, I. M., Anastassakis, E., Stanley, H. E. 1973. *Science* 182:384-86
- Asher, I. M., Rothschild, K. J., Stanley, H. E. 1974. *J. Mol. Biol.* 89:205-22
- Rothschild, K. J., Stanley, H. E. 1974. *Science* 185:616-18
- Painter, P. C., Koenig, J. L. 1975. *Biopolymers* 14:457-68
- Strekas, T. C., Adams, D. H., Packer, A., Spiro, T. G. 1974. *Appl. Spectrosc.* 28:324-27
- Shriver, D. F., Dunn, J. B. R. 1974. *Appl. Spectrosc.* 28:319-23
- Kiefer, W., Bernstein, H. J. 1971. *Appl. Spectrosc.* 25:500-1
- Woodruff, W. H., Spiro, T. G. 1974. *Appl. Spectrosc.* 28:74-75
- Mathies, R., Oseroff, A. R., Stryer, L. 1976. *Proc. Natl. Acad. Sci. USA* 73:1-5
- Callender, R. H., Doukas, A., Crouch, R., Nakanishi, K. 1976. *Biochemistry* 15:1621-28
- Van Duyne, R. P., Jeanmaire, D. L., Shriver, D. F. 1974. *Anal. Chem.* 46:213-22
- Harris, J. M., Chrisman, R. W., Lytle, F. E., Tobias, R. S. 1976. *Anal. Chem.* 48:1937-43
- Begley, R. F., Harvey, A. B., Byer, R. L., Hudson, B. S. 1974. *J. Chem. Phys.* 61:2466-67
- Nestor, J. R., Spiro, T. G., Klauminzer, G. 1976. *Proc. Natl. Acad. Sci. USA* 73:3329-32
- Tang, J., Albrecht, A. C. 1970. In *Raman Spectroscopy*, ed. H. A. Szymanski, 2: Chap. 2. New York: Plenum
- Johnson, B. B., Petricolas, W. L. 1976. *Ann. Rev. Phys. Chem.* 27:465-91
- Hirakawa, A. Y., Tsuboi, M. 1975. *Science* 188:359-61
- Inagaki, F., Tasumi, M., Miyazawa, T. 1974. *J. Mol. Spectrosc.* 50:286-303
- Heyde, M. E., Gill, D., Kilponen, R. G., Rimai, L. 1971. *J. Am. Chem. Soc.* 93:6776-80
- Lewis, A., Fager, R. S., Abrahamson, E. W. 1973. *J. Raman Spectrosc.* 1:465-70
- Lewis, A., Spoonhower, J., Bogomolni, R. A., Lozier, R. H., Stoeckenius, W. 1974. *Proc. Natl. Acad. Sci. USA* 71:4462-66
- Mendelsohn, R. 1976. *Biochim. Biophys. Acta* 427:295-301
- Oseroff, A. R., Callender, R. H. 1974. *Biochemistry* 13:4243-48
- Spiro, T. G. 1975. *Biochim. Biophys. Acta* 416:169-89
- 79a. Yamamoto, T., Palmer, G., Gill, D., Salmeen, I. J., Rimai, L. 1973. *J. Biol. Chem.* 248:5211-13
- Spiro, T. G., Burke, J. M. 1976. *J. Am. Chem. Soc.* 98:5482-89
- Perutz, M. F. 1970. *Nature* 228:726-34
- Falk, J. E. 1975. In *Porphyrins and Metalloporphyrins*, ed. K. M. Smith, pp. 317-80. Amsterdam: Elsevier
- Stein, P., Burke, J. M., Spiro, T. G. 1975. *J. Am. Chem. Soc.* 97:2304-5
- Hoard, J. L., Scheidt, W. R. 1973. *Proc. Natl. Acad. Sci. USA* 70:3919-22
- 102a. Kitagawa, T., Abe, M., Kyogoku, Y., Ogoshi, H., Watanabe, E., Yoshida, Z. 1976. *J. Phys. Chem.* 80:1181-86
- Brunner, H. 1974. *Naturwissenschaften* 61:129
- Collman, J. P., Gagne, R. R., Reed, C. A., Robinson, W. T., Rodley, G. A. 1974. *Proc. Natl. Acad. Sci. USA* 71:1326
- Kincaid, J., Nakamoto, K. 1976. *Spectrosc. Lett.* 9:19-21
- Spiro, T. G., Strekas, T. C. 1974. *J. Am. Chem. Soc.* 96:338-39
- Adar, F., Erecinska, M. 1974. *Arch. Biochem. Biophys.* 165:570-80
- Salmeen, I., Rimai, L., Gill, D., Yamamoto, T., Palmer, G., Hartzell, C. R., Beinert, H. 1973. *Biochem. Biophys. Res. Commun.* 52:1100
- Lutz, M., Breton, J. 1973. *Biochem. Biophys. Res. Commun.* 53:413-18
- Lutz, M. 1974. *J. Raman Spectrosc.* 2:417
- 110a. Ballschmitter, K., Katz, J. J. 1969. *J. Am. Chem. Soc.* 91:2661-77
- Lutz, M., Kleo, J. 1976. *Biochem. Biophys. Res. Commun.* 69:711-17
- Wozniak, W. T., Spiro, T. G. 1973. *J. Am. Chem. Soc.* 95:3402-4

113. Mayer, E., Gardiner, D. J., Hester, R. E. 1973. *Biochim. Biophys. Acta* 297:568-70; 1973. *J. Chem. Soc. Faraday Trans. 2* 69:1350-58; 1973. *Mol. Phys.* 26:783-87
114. Salama, S., Spiro, T. G. 1976. *J. Raman Spectrosc.* In press
115. Pezolet, M., Yu, T.-J., Peticolas, W. L. 1975. *J. Raman Spectrosc.* 3:55-64
116. Stein, P., Miskowski, V., Woodruff, W. H., Griffin, J. P., Werner, K. G., Gaber, B. P., Spiro, T. G. 1976. *J. Chem. Phys.* 64:2159-67
117. Yoshida, C. M., Freedman, T. B., Loehr, T. M. 1975. *J. Am. Chem. Soc.* 97:1028-32
118. Bosworth, Y. M., Clark, R. J. H., Turtle, P. C. 1975. *J. Chem. Soc. Dalton Trans.* 2027-31
119. Chottard, G., Bolard, J. 1975. *Chem. Phys. Lett.* 33:309-11
120. Long, T. V. II, Loehr, T. M., Allkins, J. R., Lovenberg, W. 1971. *J. Am. Chem. Soc.* 93:1809-11
121. Watenpaugh, K. D., Sieker, L. C., Herriott, J. R., Jensen, L. H. 1973. *Acta Crystallogr.* B29:943-56
122. Tang, S.-P. W., Spiro, T. G., Mukai, K., Kimura, T. 1973. *Biochem. Biophys. Res. Commun.* 53:869-74
123. Carter, C. W. Jr., Kraut, J., Freer, S. T., Nguyen Huu Xuong, Alden, R. A., Bartsch, R. G. 1974. *J. Biol. Chem.* 249:4212-25
124. Adman, E. T., Sieker, L. C., Jensen, L. H. 1973. *J. Biol. Chem.* 248:3987-96
125. Herskovitz, T., Averill, B. A., Holm, R. H., Ibers, J. A., Phillips, W. D., Weiher, J. F. 1972. *Proc. Natl. Acad. Sci. USA* 69:2437-41
126. DePamphilis, B. V., Averill, B. A., Herskovitz, T., Que, L. Jr., Holm, R. H. 1974. *J. Am. Chem. Soc.* 96:4159
127. Job, R. C., Bruice, T. C. 1975. *Proc. Natl. Acad. Sci. USA* 72:2478-82
128. Tang, S.-P. W., Spiro, T. G., Antanaitis, C., Moss, T. H., Holm, R. H., Herskovitz, T., Mortenson, L. E. 1975. *Biochem. Biophys. Res. Commun.* 62:1-6
129. Gaber, B. P., Miskowski, V., Spiro, T. G. 1974. *J. Am. Chem. Soc.* 96:6868-73
130. Tomimatsu, Y., Kint, S., Scherer, J. R. 1973. *Biochem. Biophys. Res. Commun.* 54:1067-74
131. Carey, P. R., Young, N. M. 1974. *Can. J. Biochem.* 52:273-80
132. Klotz, I. M., Klippenstein, G. L., Hendrickson, W. A. 1976. *Science* 192:334-44
133. Dunn, J. B. R., Shriver, D. F., Klotz, I. M. 1973. *Proc. Natl. Acad. Sci. USA* 70:2582-84
- 133a. Kurtz, D. M. Jr., Shriver, D. F., Klotz, I. M. 1976. *J. Am. Chem. Soc.* 98:5033-35
134. Dunn, J. B. R., Shriver, D. F., Klotz, I. M. 1975. *Biochemistry* 14:2689-95
135. Loehr, J. S., Freedman, T. B., Loehr, T. M. 1974. *Biochem. Biophys. Res. Commun.* 56:510-15
136. Freedman, T. B., Loehr, J. S., Loehr, T. M. 1976. *J. Am. Chem. Soc.* 98:2809-15
137. Larrabee, J. A., Ferris, N. S., Maltese, W. A., Spiro, T. G., Kerr, M. S., Woodruff, W. H. 1976. *J. Am. Chem. Soc.* 99:1979-80
138. Schugar, H. J., Solomon, E. I., Cleveland, W. L., Goodman, L. 1975. *J. Am. Chem. Soc.* 97:6442-50
139. Solomon, E. I., Hare, J. W., Gray, H. B. 1976. *Proc. Natl. Acad. Sci. USA* 73:1389-93
140. Hare, J. W., Solomon, E. I., Gray, H. B. 1976. *J. Am. Chem. Soc.* 98:3205-9
141. Markley, J. L., Ulrich, E. L., Berg, S. P., Krogmann, D. W. 1975. *Biochemistry* 14:4428-33
142. Siiman, O., Young, N. M., Carey, P. R. 1974. *J. Am. Chem. Soc.* 96:5583-85
143. Miskowski, V., Tang, S.-P. W., Spiro, T. G., Shapiro, E., Moss, T. H. 1975. *Biochemistry* 14:1244-50
144. Siiman, O., Young, N. M., Carey, P. R. 1976. *J. Am. Chem. Soc.* 98:744-48
145. Carey, P. R., Froese, A., Schneider, H. 1973. *Biochemistry* 12:2198-208
146. Kumar, K., King, R. W., Carey, P. R. 1976. *Biochemistry* 15:2195-202
147. Dupaix, A., Bechet, J.-J., Yon, J., Merlin, J.-C., Delhay, M., Hill, M. 1975. *Proc. Natl. Acad. Sci. USA* 72:4223-27
148. McFarland, J. T., Watters, K. L., Petersen, R. L. 1975. *Biochemistry* 14:624-30
149. Carey, P. R., Schneider, H. 1974. *Biochem. Biophys. Res. Commun.* 57:831-37